J Therm Anal Calorim (2017) 128:1373–1383
DOI 10.1007/s10973-016-6053-y

The synthesis and structural characterization of transition metal coordination complexes of coumarilic acid

Özge Dağlı[1] · Dursun Ali Köse[1] · Onur Şahin[2] · Zarife Sibel Şahin[3]

Received: 23 September 2016 / Accepted: 9 December 2016 / Published online: 16 January 2017

Abstract The coumarilate ($coum^-$) complexes of Co^{II}(**1**), Ni^{II}(**2**) Cu^{II}(**3**) and Zn^{II}(**4**) were synthesized and characterized by elemental analysis, magnetic susceptibility, solid-state UV–Vis, FTIR spectra, thermoanalytical TG–DTG/DTA and single-crystal X-ray diffraction methods. It was found that all of the complex structures have 2 mol ($coum^-$) ligand bonded as monoanionic monodentate in the structures of **1** and **2** while they were coordinated to metal cations as monoanionic bidentate in the complexes **3** and **4**. There was not any hydrate water in the metal complexes. The complexes of **1** and **2** have four moles of aqua ligand, and the other complexes have two moles. Thermal decomposition of each complex starts with dehydration, and then the decomposition of organic parts goes. The thermal dehydration of the complexes takes place in one (for the compounds of **2**, **3**, **4**) or two (for the compound **1**) steps. The decomposition mechanism and the thermal stability of the complexes under investigation were determined on the basis of their structures. Metal oxides were obtained as the final decomposition product.

Keywords Coumarilate · Metal complexes · Thermal analysis · Crystal structure · Structural analysis

✉ Dursun Ali Köse
dalikose@hitit.edu.tr

[1] Department of Chemistry, Hitit University, 19040 Ulukavak/Çorum, Turkey

[2] Scientific and Technological Research Application Center, Sinop University, 57000 Sinop, Turkey

[3] Department of Energy Systems Engineering, Sinop University, 57000 Sinop, Turkey

Introduction

The cyclic compounds having a heteroatom and the derivatives have been used in the field of medicine and agriculture. The coumarilic acid having benzofuran and derivatives are the examples used in these and also in various fields of our life [1]. Coumarilic acid (1-benzofuran-2-carboxylic acid) is formed by the combination of 2-furan carboxylic acid ring having benzene nucleus.

Other name for this compound is *benzofuran-2-carboxylic acid* having the empirical formula of C9H6O3 and the molecular mass of 162.14 g mol^{-1}. The melting point of benzofuran-2-carboxylic acid ranges from 193 to 196 °C.

It is well known that many of the heterocyclic compounds having oxygen show significant biological properties such as antiarrhythmic, spasmolytic, antiviral, anticancer, antifungal and anti-inflammatory activity [2–8]. Currently, there are many pharmaceutical applications on the use of natural or synthetic derivatives [9, 10]. Although there have been numerous studies on derivatives of coumarilic acid [11–13], the number of studies on metal complexes has been limited. In the study conducted by Kose et al. [14], the synthesis of Co^{II}- and Zn^{II}-coumarilate–nicotinamide mixed ligand complexes were performed and characterized.

Drzewiecki et al. [15] have synthesized the Cu(II) complexes by electrochemical methods. Three different coumarilic acid derivatives were used for the complex formation. These are complexes of 7-acetyl-6-methoxy-3-methyl-benzo[b]furan-2-carboxylic acid (HL1), 7-acetyl-5-bromo-6-hydroxy-3-methyl-benzo[b]furan-2-carboxylic acid (HL2) and 6-acetyl-5-hydroxy-2-methyl-benzo[b]furan-3-carboxylic acid (HL3) [16–18].

Scheme 1 Synthesis reaction of metal–coumarilate coordination compounds

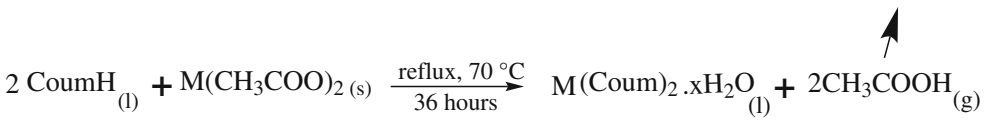

CoumH: 1-benzofuran-2carboxylic acid
Coum: 1-benzofuran-2carboxylato
M: Co, Ni, Cu, Zn
x: 2,4

Table 1 Analytical data of metal complexes

Complex	MW/g mol^{-1}e	Yield	Content/% exp. (calc.)		Colour	Decomp. temp/°C	$\mu_{eff.}$ (BM)
			C	H			
$[Co(C_9H_5O_3)2(H_2O)4]$ C18H18CoO10	453.26	85	47.78 (47.70)	3.63 (4.00)	Purple	127	4.42
$[Ni(C_9H_5O_3)2(H_2O)4]$ C18H18NiO10	453.02	88	47.83 (47.72)	3.82 (4.00)	Green	96	3.63
$[Cu(C_9H_5O_3)2(H_2O)2]$ C18H14CuO8	421.84	94	51.66 (51.25)	3.61 (3.35)	Blue	125	1.74
$[Zn(C_9H_5O_3)2(H_2O)2]$ C18H14O8Zn	423.68	89	49.89 (51.03)	3.47 (3.33)	White	181	Dia.

Table 2 FTIR spectra of metal–coumarilate mixed ligand complexes (cm^{-1})

Groups	Co^{II}(**1**)	Ni^{II}(**2**)	Cu^{II}(**3**)	Zn^{II}(**4**)
$\nu(OH)H_2O$	3550–2900	3550–2900	3550–2900	3400–2800
$\nu(=C–H)_{ar}$	3028	3022	3025	3030
$\nu(C=C)_{ar}$	1705	1708	1692	1695
$\nu(C=O)_{carbonyl}$	1591	1593	1599	1597
$\nu(COO-)_{asym}$	1549	1552	1573	1576
$\nu(COO-)_{sym}$	1405	1408	1398	1399
$\Delta\nu_{as-s}$	144	144	175	177
$\delta(OH)H_2O$	1488	1485	1475	1477
$\nu(C–O)_{carboxyl}$	1343	1344	1338	1328
$\nu(C_9–O_1–C_1)$	1251/1181	1253/1183	1250/1184	1254/1185
$\nu_{(ring)}$	1111–831	1109–832	1106–829	1114–856
ν(M–O–)	428	429	432	427
ν(M–O=)	–	–	471	487

Within the scope of the complexation reactions of coumarilic acid, the synthesis and characterization of coordination compounds having Ni^{II}, Co^{II}, Zn^{II}, Mn^{II} [8, 11], Cu^{II} [10], Ce^{III}, Nd^{III} [19], La^{III} [20, 21], Dy^{III}, Er^{III}, Eu^{III}, Gd^{III}, Tb^{III}, Sm^{III} [22, 23] were studied. Despite the many studies about the metal complexes of coumarilic acid, there are a limited number of studies on the crystal structures [10, 11, 14, 19]. Because the coumarilic acid has broad physiological and biological effects, it plays very important role in medicinal inorganic chemistry [24, 25].

In this study, the coordination compounds of coumarilic acid having Co^{II}, Ni^{II}, Cu^{II} and Zn^{II} transition metals were synthesized. The molecular structures of the complexes synthesized were determined via elemental analysis, Fourier transform infrared spectroscopy (FTIR), thermogravimetric analysis (TG/DTA), single-crystal X-ray diffraction diffractometry (SC-XRD), solid ultraviolet–visible spectroscopy (UV–Vis), magnetic susceptibility and melting point detection methods.

Materials and methods

The chemicals $Co(CH_3COO)2.4H_2O$, $Ni(CH_3COO)2.4H_2O$, $Cu(CH_3COO)2.H_2O$, $Zn(CH_3COO)2.2H_2O$ and coumarilic acid used in the synthesis of complexes were obtained from the company *Sigma-Aldrich*. Elemental analysis (C, H, N) was being carried out by Standard Methods. Magnetic susceptibility measurements were performed at room temperature using a Sherwood Scientific MXI model Gouy magnetic balance. IR spectra were recorded in the 4000–400 cm^{-1} region with a PerkinElmer Spectrum One FTIR spectrophotometer using KBr pellets. Thermal analyses (TG, DTA) were performed by the Shimadzu DTG-60H system, in a dynamic nitrogen atmosphere (100 mL min^{-1}) at a heating rate of 10 °C min^{-1}, in platinum crucibles as the sample vessel, using α-Al_2O_3 as a reference.

Experimental

In the first step of the synthesis, coumarilic acid of 0.005 mol was dissolved in the solution of $EtOH/H_2O$ in 50:50 (v/v). The acetate salts of Co, Ni, Cu and Zn metals (0.0025 mol of each) were added to the solution obtained stirred in reflux at 70 °C for 36 h. In the reaction, the reference stoichiometric ratio was 1:2 (metal/ligand). The emission of CH_3COOH (acetic acid) gas was observed. The

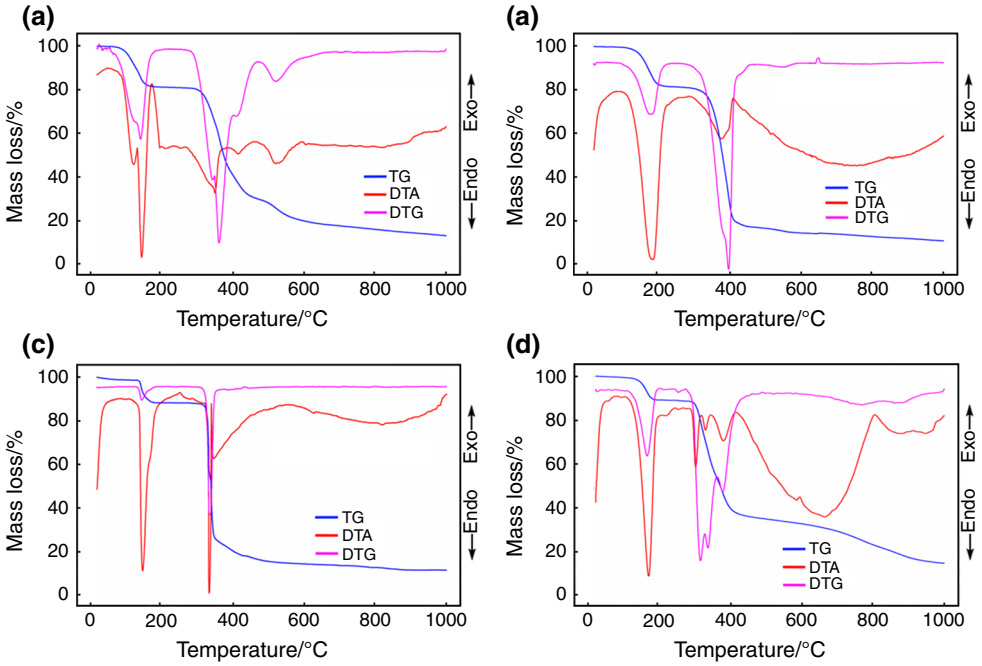

Fig. 1 Thermal analysis curves of compounds, **a** $[Co(C_9H_5O_3)2(H_2O)4]$, **b** $[Ni(C_9H_5O_3)2(H_2O)4]$, **c** $[Cu(C_9H_5O_3)2(H_2O)2]$, **d** $[Zn(C_9H_5O_3)2(H_2O)4]$

heating and stirring were continued until no acetic acid odour was smelled.

The final solution was allowed to crystallize at atmospheric pressure at room temperature. The crystals were formed in approximately 2–4 weeks collected by filtration.

The metal/ligand ratio was determined as 1:2 for the compounds (Co, Ni, Cu and Zn transition metal complexes). The synthesis reaction is shown in Scheme 1.

Results and discussion

Elemental analysis results of metal–coumarilate complexes are given in Table 1. The results of melting points, magnetic susceptibility, colours and the yield determination are also given in the table.

FTIR analysis

The significant stretching and bending vibrations obtained using FTIR spectroscopy are summarized in Table 2. The coumarilic acid attached to the structure as a ligand bounded to the metal cations. The carboxyl group peaks of coumarilic acid were shifted to the right due to the coordination to the metal cations. Therefore, there are stretching vibrations observed for the complexes of Co^{II}, Ni^{II}, Cu^{II} and Zn^{II} originating from the carboxylic acid groups at 1591, 1593, 1599 and 1597 cm^{-1}, respectively.

The strong and broaden band observed near 3350–2800 cm^{-1} in the spectrum is due to the presence of –OH groups. Aromatic C–H stretching vibrations in the complexes result a peak in between 3022 and 3030 cm^{-1}. The asymmetric and symmetric absorption bands of COO^- correspond to the stretching vibrations at 1549–1576 and 1398–1408 cm^{-1}, respectively. The absorption bands corresponding to the metal–oxygen (M–O and M–O=) bindings, which is a base for complexes, provide stretching vibrations at 428 cm^{-1} for Co^{II}, 429 cm^{-1} for Ni^{II}, 432 and 471 cm^{-1} for Cu^{II} and 427 and 487 cm^{-1} for Zn^{II}.

Thermal analysis

Thermal analysis curves (TG, DTG and DTA) of the complexes are shown in Fig. 1a–d. The decomposition steps and leaving groups are summarized in Table 3.

It can be observed from the DTG plot of the Co^{II} mixed ligand (1) complex that it goes degradation in three steps corresponding to the maximum temperatures of 128, 148 and 329; 387; 479 °C. The first degradation step is the removal of 2 of 4 mol of water bonded to the metal via coordinated covalent bond in the coordination sphere.

$$[Co(C_9H_5O_3)_2(H_2O)_4]_{(s)} \xrightarrow{84\text{-}133^{o}C} [Co(C_9H_5O_3)_2(H_2O)_2]_{(s)} + 2H_2O_{(g)} \uparrow \quad \text{R-1}$$

The other 2 mol of water remaining in the coordination sphere during the degradation step at 148 °C was completely removed at the temperature range of 134–215 °C.

$$[Co(C_9H_5O_3)_2(H_2O)_2]_{(s)} \xrightarrow{134\text{-}215^{o}C} [Co(C_9H_5O_3)_2]_{(s)} + 2H_2O_{(g)} \uparrow \quad \text{R-2}$$

Table 3 Thermal analysis data of metal–coumarilate complexes

Complex	Temp. range/°C	DTA_{max}/°C	Removed group	Mass loss/%		Remained prod./%		Decomp. product	Colour
				Exp.	Theor.	Exp.	Theor.		
$[Co(C_9H_5O_3)_2(H_2O)_4]$									Pink
$C_{18}H_{18}CoO_{10}$									
1	84–133	128	$2H_2O$	8.02	7.94				
453.26 g mol^{-1}									
2	134–215	148	$2H_2O$	7.92	7.94				
3	275–767	329, 387, 479	$C_9H_5O_2$; $C_9H_5O_3$	64.26	67.53	19.80	16.53	CoO	Black
$[Ni(C_9H_5O_3)_2(H_2O)_4]$									Green
$C_{18}H_{18}NiO_{10}$									
1	99–217	168	$4H_2O$	15.85	15.89				
453.02 g mol^{-1}									
2	238–780	342, 362, 745	$C_9H_5O_2$; $C_9H_5O_3$	66.82	67.56	17.13	16.49	NiO	Black
$[Cu(C_9H_5O_3)_2(H_2O)_2]$									Blue
$C_{18}H_{14}CuO_8$									
1	35–86	63	$H_2O_{(moisture)}$	0.90	–				
421.84 g mol^{-1}									
2	120–167	132, 151	$2H_2O$	8.82	8.53				
3	267–860	301, 313, 715	$C_9H_5O_2$; $C_9H_5O_3$	68.86	72.56	21.42	18.85	CuO	Black
$[Zn(C_9H_5O_3)_2(H_2O)_2]$									White
$C_{18}H_{14}O_8Zn$									
1	36–114	90	$H_2O_{(moisture)}$	0.70	–				
423.68 g mol^{-1}									
2	116–200	166	$2H_2O$	8.56	8.50				
3	281–892	301, 328, 378, 663, 879	$C_9H_5O_2$; $C_9H_5O_3$	69.12	72.29	21.68	19.21	ZnO	Grey

The coumarilate ligands in the degradation step at 329; 387; 479 °C were removed by degradation at the temperature range of 275–767 °C. The black coloured CoO compound remained as a decomposition product.

$$[Co(C_9H_5O_3)_2]_{(s)} \xrightarrow{275\text{-}767^{\circ}C} CoO_{(s)} + C_9H_5O_{3(decomp.)} + C_9H_5O_{2(decomp.)} \quad \text{R-3}$$

It can be seen in the DTA curves of the complex (2) having Ni^{II} mixed ligand that it decomposes in two steps corresponding to the maximum temperatures of 168 and 342; 362; 745 °C. The first decomposition step is the removal of 4 mol of water from the structure within the coordination sphere.

$$[Ni(C_9H_5O_3)_2(H_2O)_4]_{(s)} \xrightarrow{99\text{-}217^{\circ}C} [Ni(C_9H_5O_3)_2]_{(s)} + 4H_2O_{(g)} \uparrow \quad \text{R-4}$$

The coumarilate ligands in the degradation step at 342; 362; 745 °C were removed by degradation at the temperature range of 238–780 °C. The black coloured NiO compound remained as a decomposition product.

$$[Ni(C_9H_5O_3)_2]_{(s)} \xrightarrow{238\text{-}780^{\circ}C} NiO_{(s)} + C_9H_5O_{3(decomp.)} + C_9H_5O_{2(decomp.)} \quad \text{R-5}$$

It can be seen in the DTG curves of the complex (3) having Cu^{II} mixed ligand that it decomposes at three steps corresponding to the maximum temperatures of 63, 132; 151 and 301; 313; 715 °C. The first decomposition step was the removal of moisture from the structure at the temperature of 35–86 °C. The 2 mol of water within the coordination sphere in the decomposition step at 132; 151 °C was removed at the temperature range of 120–167 °C.

$$[Cu(C_9H_5O_3)_2(H_2O)_2]_{(s)} \xrightarrow{120\text{-}167^{\circ}C} [Cu(C_9H_5O_3)_2]_{(s)} + 2H_2O_{(g)} \uparrow \quad \text{R-6}$$

The coumarilate ligands in the degradation step at 301; 313; 715 °C were removed by degrading at the temperature range of 267–860 °C. The black coloured CuO compound remained as a decomposition product.

Table 4 Crystal data of $[Co(C_9H_5O_3)2(H_2O)4]$, $[Ni(C_9H_5O_3)2(H_2O)4]$ and $[Zn(C_9H_5O_3)2(H_2O)2]$ complexes

Crystal data			
Chemical formula	$C_{18}H_{18}CoO_{10}$ (**1**)	$C_{18}H_{18}NiO_{10}$ (**2**)	$C_{18}H_{14}O_8Zn$ (**4**)
M_r	453.25	453.03	423.66
Crystal system, point group	Monoclinic, $P2_1$	Monoclinic, $P2_1$	Monoclinic, $C2$
Temp./K	296	296	296
a/Å	4.9946 (4)	4.9517 (7)	12.0604 (13)
b	29.992 (3)	30.057 (4)	5.0281 (5)
c	6.3558 (6)	6.2956 (10)	13.6345 (14)
β/°	102.103 (3)	101.938 (4)	90.909 (4)
V/Å^3	930.92 (14)	916.7 (2)	826.70 (15)
Z	2	2	2
Beam source	Mo-K$_\alpha$/0.71073	Mo-K$_\alpha$/0.71073	Mo-K$_\alpha$/0.71073
μ/mm^{-1}	0.98	1.12	1.53
Crystal size/mm	0.35 × 0.30 × 0.27	0.18 × 0.15 × 0.10	0.30 × 0.18 × 0.10
d/g/cm^3	1.617	1.641	1.702
$\theta_{max.}$/°	28.4	27.3	28.3
Colour	Pink	Green	Colourless
T_{min}, T_{max}	0.559, 0.746	0.552, 0.746	0.506, 0.746
Measurable, observable [$I > 2\sigma(I)$] and free reflection number	11,529, 3443, 3356	20,425, 4389, 3642	6469, 1949, 1879
R_{int}	0.047	0.069	0.045
$(\sin\theta/\lambda)_{max}$/Å^{-1}	0.617	0.667	0.667
$R[F^2 > 2\sigma(F^2)]$, $Wr(F^2)$, S	0.050, 0.117, 1.17	0.100, 0.236, 1.16	0.039, 0.089, 1.16
Reflection number	3443	4389	1949
Parameter number	270	269	130
$\Delta\rho_{max}$, $\Delta\rho_{min}$/e Å^{-3}	1.31, −0.80	1.78, −1.92	0.67, −0.68
Absolute structure	Asymmetric geminal	Asymmetric geminal	Asymmetric geminal
Absolute structure parameter	0.46 (4)	0.31 (7)	0.14 (2)

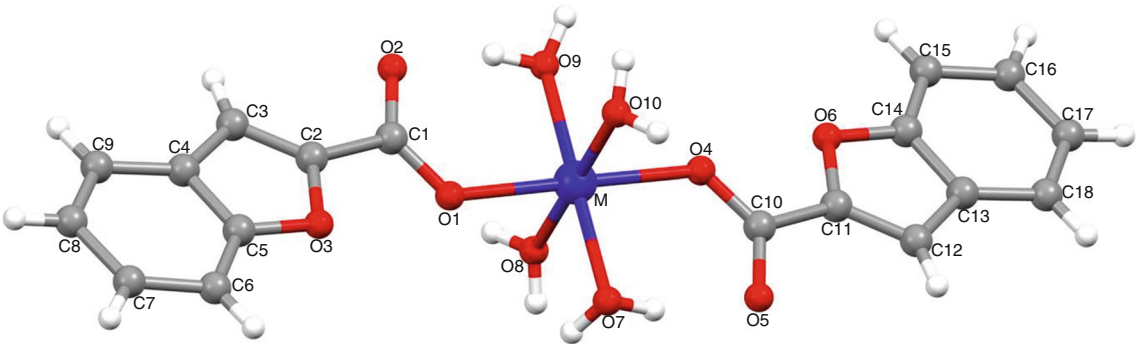

Fig. 2 Molecular structure of complexes **1** and **2** (M=Co(II) in **1** and Ni(II) in **2**) showing the atom-numbering scheme

$$[Cu(C_9H_5O_3)_2]_{(s)} \xrightarrow{267\text{-}860\ ^\circ C} CuO_{(s)} + C_9H_5O_{3(decomp.)} + C_9H_5O_{2(decomp.)} \quad \text{R-7}$$

It can be seen in the DTG curves of the complex (4) having the Zn^{II} mixed ligand that it decomposes in three steps corresponding to the maximum temperatures of 90, 166 and 301; 328; 378; 663; 879 °C. The first decomposition step was the removal of moisture from the structure at the temperature of 36–114 °C. The 2 mol of water within the coordination sphere in the decomposition step at 166 °C was removed at the temperature range of 116–200 °C.

Table 5 Selected bond distances and angles for complexes **1**, **2** and **4** (Å, °)

$[Co(C_9H_5O_3)_2(H_2O)_4]$					
O1-Co1	2.129 (6)	O4-Co1	2.124 (6)	Co1-O9	2.074 (5)
Co1-O8	2.094 (6)	Co1-O10	2.095 (6)	Co1-O7	2.097 (5)
O9-Co1-O8	90.9 (2)	O9-Co1-O10	88.4 (2)	O9-Co1-O7	179.5 (3)
O8-Co1-O10	179.3 (3)	O8-Co1-O7	89.0 (2)	O10-Co1-O7	91.6 (2)
$[Ni(C_9H_5O_3)_2(H_2O)_4]$					
O1-Ni1	2.103 (11)	O4-Ni1	2.093 (12)	Ni1-O8	2.012 (9)
Ni1-O10	2.043 (10)	Ni1-O7	2.058 (11)	Ni1-O9	2.068 (12)
O8-Ni1-O10	179.4 (5)	O8-Ni1-O7	89.4 (4)	O10-Ni1-O7	90.3 (4)
O8-Ni1-O9	88.5 (5)	O10-Ni1-O9	91.9 (4)	O7-Ni1-O9	177.0 (5)
$[Zn(C_9H_5O_3)_2(H_2O)_2]$					
O1-Zn1	2.0170 (19)	O2-Zn1	2.523 (2)	Zn1-O4	1.979 (2)
O1-Zn1-O2	56.67 (3)	O2-Zn1-O4	82.24 (2)	O4-Zn1-O1	135.18 (8)

$$[Zn(C_9H_5O_3)_2(H_2O)_2]_{(s)} \xrightarrow{116\text{-}200^{\circ}C} [Zn(C_9H_5O_3)_2]_{(s)} + 2H_2O_{(g)} \quad \text{R-8}$$

The coumarilate ligands in the degradation step at 301; 328; 378; 663; 879 °C were removed by degradation at the temperature range of 281–892 °C. The grey coloured ZnO compound remained as a decomposition product.

$$[Zn(C_9H_5O_3)_2]_{(s)} \xrightarrow{281\text{-}892^{\circ}C} ZnO_{(s)} + C_9H_5O_{3(decomp.)} + C_9H_5O_{2(decomp.)} \quad \text{R-9}$$

All of the last decomposition products related metal oxides were identified by FTIR spectroscopy [26].

Single X-ray diffraction analysis

Suitable crystals of **1**, **2** and **4** were selected for data acquisition, which was performed on a Bruker D8-QUEST diffractometer equipped with a graphite monochromatic Mo-K_α radiation. The structures were determined by direct methods using the software SHELXS-97 [27] and refined by full-matrix least-squares methods on F^2 using the software SHELXL-97 [27] within the software WINGX [28]. All atoms except for hydrogen were refined with anisotropic parameters. The H atoms bonded to C atoms were located in simulation using a different maps and then treated as riding atoms having C–H distances of 0.93 Å. The H atoms of water were located in simulation using a different map refined freely. Molecular diagrams were created using the software MERCURY [29]. Supramolecular analyses were conducted. The diagrams were prepared with the aid of the software PLATON [30]. Details of data acquisition and crystal structure determinations are given in Table 4.

Table 6 Hydrogen bond distances of complexes with **1**, **2** and **4** geometry (Å, °)

D–H···*A*	*D*–H	H···*A*	*D*···*A*	*D*–H···*A*
$[Co(C_9H_5O_3)_2(H_2O)_4]$				
O7–H7*B*···O4^{i}	0.84 (3)	2.20 (4)	3.007 (8)	161 (7)
O7–H7*A*···O5	0.83 (3)	1.82 (3)	2.635 (8)	164 (8)
O8–H8*A*···O5^{ii}	0.83 (3)	1.84 (3)	2.649 (8)	164 (8)
O8–H8*B*···O4^{i}	0.82 (3)	2.35 (6)	3.033 (9)	141 (8)
O8–H8*B*···O6^{i}	0.82 (3)	2.37 (6)	3.016 (8)	136 (8)
O9–H9*A*···O2	0.83 (3)	1.84 (4)	2.623 (8)	156 (8)
O9–H9*B*···O1^{iii}	0.82 (3)	2.50 (8)	3.004 (8)	120 (7)
O9–H9*B*···O8^{iii}	0.82 (3)	2.53 (6)	3.089 (9)	127 (6)
O10–H10*A*···O1^{iii}	0.81 (3)	2.21 (4)	2.988 (10)	161 (9)
O10–H10*A*···O3^{iii}	0.81 (3)	2.60 (8)	3.079 (8)	119 (8)
O10–H10*B*···O2^{iv}	0.83 (3)	1.85 (3)	2.660 (8)	166 (9)
$[Ni(C_9H_5O_3)_2(H_2O)_4]$				
O7–H7*B*···O5^{i}	0.85 (3)	1.85 (6)	2.658 (14)	160 (15)
O7–H7*A*···O1	0.83 (3)	2.47 (14)	2.966 (13)	120 (13)
O8–H8*B*···O1^{iii}	0.83 (3)	2.48 (14)	3.000 (15)	122 (14)
O8–H8*B*···O7^{iii}	0.83 (3)	2.58 (10)	3.148 (14)	127 (11)
O8–H8*A*···O2	0.83 (3)	1.96 (16)	2.601 (15)	133 (19)
O9–H9*A*···O2^{iv}	0.84 (3)	1.83 (4)	2.668 (15)	173
O9–H9*B*···O1^{iii}	0.83 (3)	2.19 (9)	2.912 (17)	146 (14)
O9–H9*B*···O10^{iii}	0.83 (3)	2.60 (14)	3.028 (16)	114 (12)
O10–H10*A*···O4^{ii}	0.84 (3)	2.33 (13)	3.019 (18)	140 (18)
O10–H10*A*···O9^{ii}	0.84 (3)	2.33 (11)	3.028 (16)	141 (16)
O10–H10*B*···O8^{v}	0.83 (3)	2.57 (13)	3.193 (11)	132 (14)
$[Zn(C_9H_5O_3)_2(H_2O)_2]$				
C3–H3···O4^{i}	0.93	2.60	3.381 (5)	142
O4–H4*A*···O1^{ii}	0.83 (2)	1.98 (3)	2.764 (4)	158 (6)
O4–H4*B*···O2^{iii}	0.82 (2)	1.85 (3)	2.666 (4)	172 (7)
C5–H5···O3	0.93	2.60	3.381 (5)	142

Symmetry codes: (i) $x + 1, y, z$; (ii) $x, y, z - 1$; (iii) $x - 1, y, z$; (iv) $x, y, z + 1$

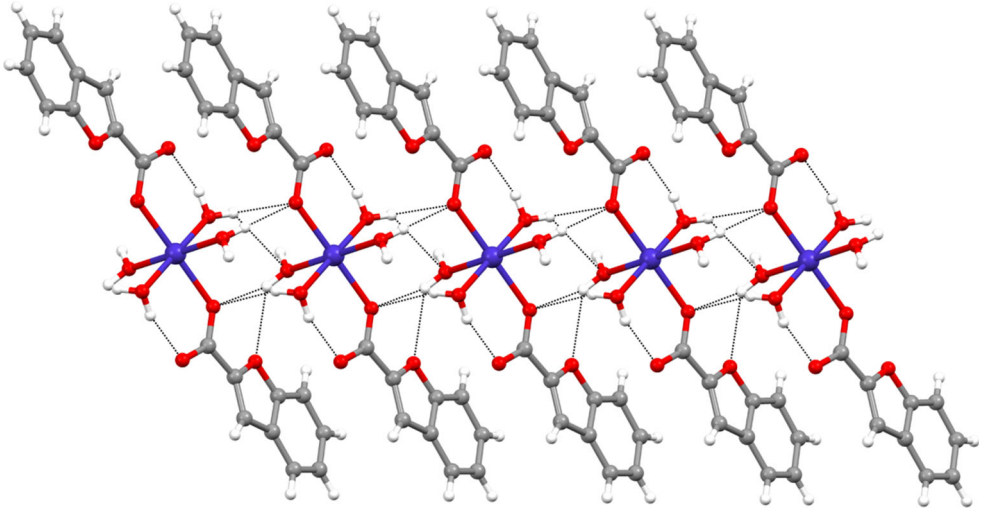

Fig. 3 Formation of edge-fused $R_1^2(5)$, $R_2^1(6)$, $R_2^2(6)$ and $R_2^2(8)$ rings in **1** and **2**

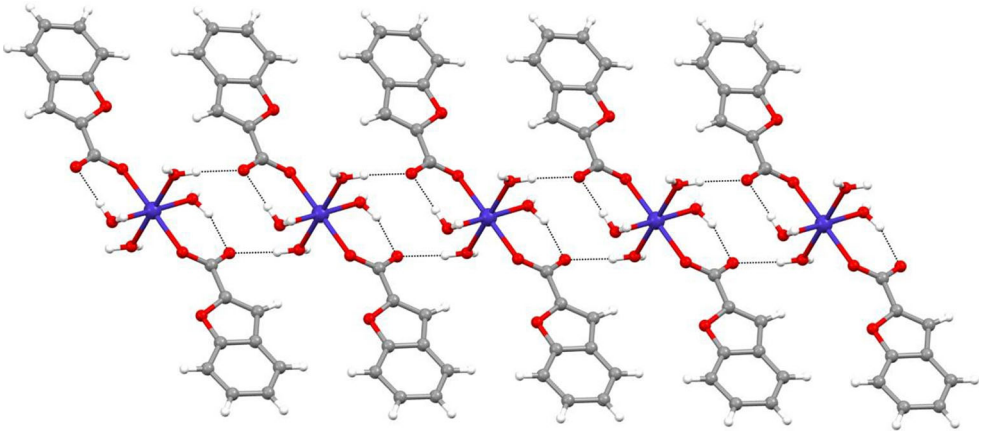

Fig. 4 Formation of edge-fused $R_2^2(12)$ rings in **1** and **2**

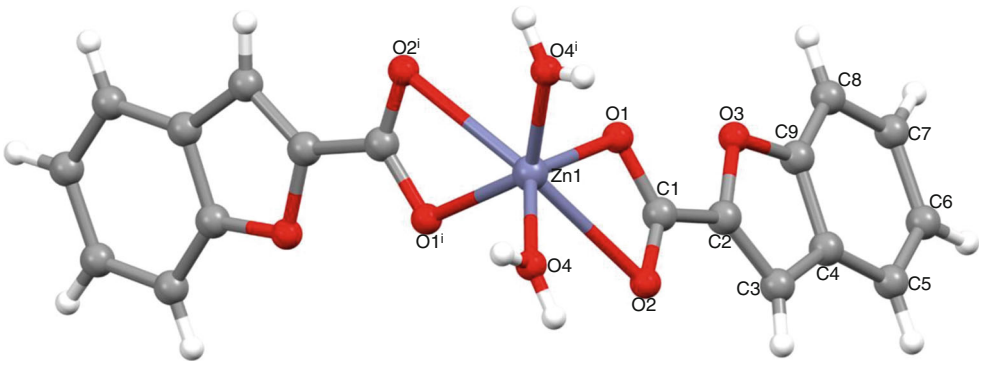

Fig. 5 Molecular structure of complex **4** showing the atom-numbering scheme [(i) $-x + 1$, y, $-z + 1$]

The molecular structures of complexes **1–2** are shown in Fig. 2 with the atom-numbering schema, and selected bond and bond angles are summarized in Table 5. The asymmetric units of **1–2** have one M(II) ion [M(II) = Co(II) in **1** and Ni(II) in **2**], two coumarilic acid ligands and four aqua ligands. Each M(II) ion was coordinated by two oxygen atoms of two different coumarilic acid ligands and four oxygen atoms of aqua ligands. The coordination geometry around the M(II) ion M(II) ion [M(II) = Co(II) in **1** and Ni(II) in **2**] can be described as the distorted octahedral. The M–$O_{carboxyl}$ bond lengths are 2.124 (6) and 2.129 (6) Å in **1** and 2.093 (12) and 2.103 (11) Å in **2**. The M–$O_{(aqua)}$ bond lengths are ranged between 2.074 (5)–2.097 (5) Å in **1** and 2.012 (9)–2.068 (12) Å in **2**.

Compounds of **1–2** are attached to the sheets by a combination of O–H···O hydrogen bonds (Table 6). Strong hydrogen bonds were observed between carboxyl groups and aqua oxygen atoms, with the O···O distances ranging

Fig. 6 An infinite 2D layer in **4**

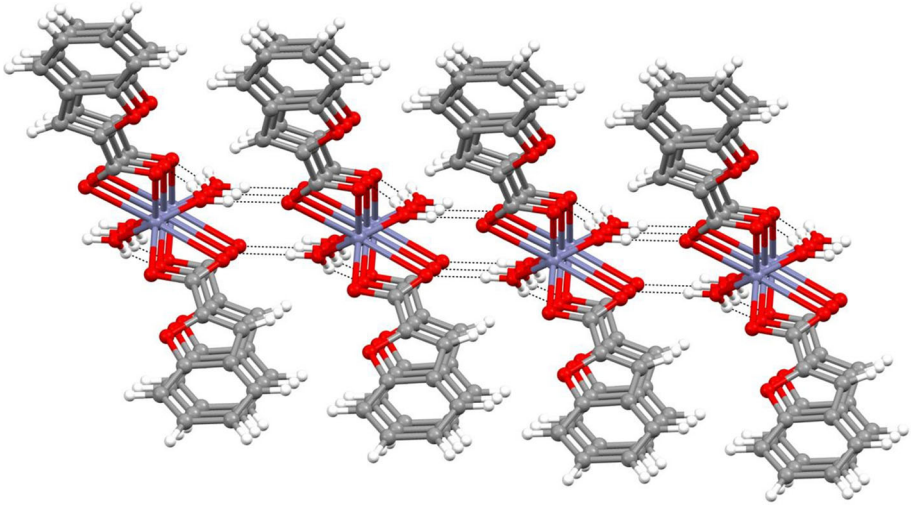

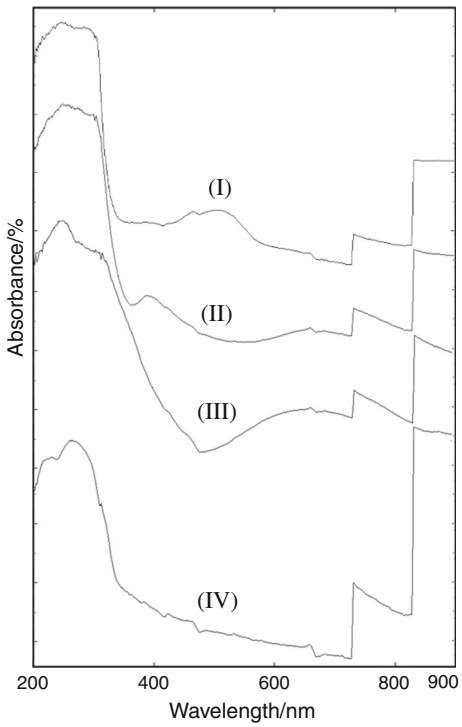

Fig. 7 UV–Vis–NIR Spectra of complexes **1**–**4**

from 2.623 (8) to 3.089 (9) Å for complex **1** and from 2.601 (15) to 3.193 (11) Å for complex **2**. The combination of O–H···O hydrogen bonds produce edge-fused $R_1^2(5)$, $R_2^1(6)$, $R_2^2(6)$ and $R_2^2(8)$ rings running parallel to the [100] direction (Fig. 2). Similarly, a combination of O–H···O hydrogen bonds produces edge-fused $R_2^2(12)$ rings running parallel to the [001] direction (Fig. 3). All of these intermolecular interactions give two-dimensional framework results. The formation of edge-fused $R_2^2(12)$ rings in **1** and **2** (Fig. 4).

The molecular structure schema of complex **4** with atom labelling is shown in Fig. 5, and the selected bonds and bond angles are summarized in Table 5. The asymmetric unit of complex **4** contains one Zn(II) ion, one coumarilic acid and one aqua ligand. The Zn(II) ion was located in the centre of the symmetry and coordinated to four oxygen atoms of two different coumarilic acid ligands and two oxygen atoms of aqua ligands. The Zn(II) ion was coordinated by two oxygen atoms of two different coumarilic acid ligands and four oxygen atoms of aqua ligands. The coordination geometry around the Zn(II) ion can be described as the distorted octahedral. The $Zn–O_{carboxyl}$ bond lengths are 2.0170 (19) and 2.523 (2) Å, while the $Zn–O_{aqua}$ bond length is 1.979 (2) Å.

The complex **4** was attached to the sheets by the combination of O–H···O and C–H···O hydrogen bonds

Table 7 UV–Vis spectra of metal–coumarilate mixed ligand complexes

Transitions	Comp.			
	$C_{18}H_{18}CoO_{10}$ (octahedral)	$C_{18}H_{18}NiO_{10}$ (octahedral)	$C_{18}H_{14}CuO_8$ (octahedral)	$C_{18}H_{14}O_8Zn$ (octahedral)
d–d	512.35 ($^4T_{1g} \rightarrow {}^4T_{2g}$) (F)	817.22 ($^3A_{2g} \rightarrow {}^3T_{1g}$) (P)	887.62–501.13, 709.71 ($^2E_g \rightarrow {}^2T_{2g}$)	–
d–d	463.12 ($^4T_{1g} \rightarrow {}^4T_{1g}$) (P)	654.76 ($^3A_{2g} \rightarrow {}^3T_{1g}$) (F)		
		395.67 ($^3A_{2g} \rightarrow {}^3T_{2g}$) (F)		
$M \rightarrow L$	252.49	253.11	244.79	–
$L \rightarrow M$	–	–	–	268.57

(Table 6). The O4 atom of water in the compounds at (x, y, z) acted as hydrogen-bond donor, via atoms H2A and H2B, to atoms $O2^{iii}$ and $O1^{iv}$, so forming $R_3^3(10)$ rings [(iii) $-x + 3/2$, $y + 1/2$, $-z + 1$ and (iv) $-x + 1$, $y + 1$, $-z + 1$]. The combination of these hydrogen bonds produces two-dimensional framework result (Fig. 6).

The solid-state UV–Vis spectroscopy

The electronic transition values of metal–coumarilate mixed ligand complexes synthesized in this study were derived from the spectra pattern obtained using solid-state visible spectroscopy (UV–Vis) in the wavelength interval of 900–200 nm (Fig. 7). The data obtained from the spectroscopic data are summarized in Table 7.

According to the solid-state UV–Vis spectroscopy results, *d–d* transitions attributed to Co^{II}(**1**) complexes were observed at 512.35 ($^4T_{1g} \rightarrow {}^4T_{2g}$) (F) and 463.12 nm ($^4T_{1g} \rightarrow {}^4T_{1g}$) (P). The spin-allowed *d–d* transition belonging to Ni^{II}(**2**) complex was observed in the wavelengths of 817.22 nm ($^3A_{2g} \rightarrow {}^3T_{1g}$) (P), 654.76 nm ($^3A_{2g} \rightarrow {}^3T_{1g}$) (F) and 395.67 nm ($^3A_{2g} \rightarrow {}^3T_{2g}$) (F). Therefore, these transition bands show the cleavage of *d* orbitals of Ni^{II} metal cations supporting the octahedral geometry. The multiple absorption bands owned by Cu^{II}(**3**) complex were formed by band-overlapping. It has a broaden view in a wide wavelength range of 887.62–501.13 nm. In the light of these spectral data, it is thought that Cu^{2+} metal cations promote the "pseudo-octahedral" structure under the influence of the Jahn–Teller effect. The maximum absorption band of the broad spectrum of the Cu^{II}(**3**) complex corresponds approximately to the wavelength of 709.71 nm ($^2E_g \rightarrow {}^2T_{2g}$). With respect to the magnetic susceptibility values, because the *d* orbitals in the last orbital of the metal cation in the Zn^{II}(**4**) complex with diamagnetic properties were fully occupied, there was no any *d–d* electronic transition observed for any possible octahedral cleavage.

The absorption bands with high intensity observed in low wavelengths are not *d–d* transitions, but special to metal → ligand charge transfer transitions with higher energy.

While absorption bands in 252.49 nm for Co^{II}(**1**) complex, 253.11 nm for Ni^{II}(**2**) complex, 244.79 nm Cu^{II}(**3**) complex are owned by metal → ligand ($M \rightarrow L$) transitions, the intense band observed in 268.57 nm for Zn^{II}(**4**) complexes is owned by ligand → metal ($L \rightarrow M$) charge transfer. These data were suitable with the literature [31–33].

Conclusions

In this study, the mixed ligand coordination compounds of cobalt(II), nickel(II), copper(II) and zinc(II) transition metals and coumarilate were synthesized. According to the elemental analysis results of complexes, the metal/ligand ratio was determined as 1:2.

According to structural analysis results obtained, the complexes **1** and **2**, structures of which were identified, were determined as isostructural. Co and Ni cations in the structures have completed their octahedral sphere with four water atoms bonded as a ligand by entering the coordination sphere. The existence of octahedral sphere was proved by the data obtained using both solid-state UV–Vis–NIR spectrophotometer and magnetic susceptibility test. The single crystal structure of the compound having Zn^{II} cation was the one only identified among others. The compliance between the spectroscopic results and the structure number **3** proves that these two compounds are isostructural. The geometries of these structures were also determined as distorted octahedral. Two moles of monoanionic coumarilate ligands were coordinated to the metal in the coordination sphere. However, this coordination occurs as bidentate. Besides coumarilate ligands, two moles of water have completed the octahedral geometry by coordination with the metals. Moreover, the octahedral sphere was also proved by the data obtained using both solid-state UV–Vis–NIR spectrophotometer and magnetic susceptibility test.

The mono- and bidentate binding features of coumarilate ligands were also proved by FTIR spectra. The difference between $\nu(COO-)_{asym}$ and $\nu(COO-)_{sym}$ gives an idea about the binding behaviour of carboxylate whether mono- or bidentate. If the difference between these two stretching vibrations is greater than 150 cm^{-1}, the binding is monoanionic bidentate; if smaller, the binding is monoanionic monodentate [23, 26, 33–35]. According to Table 2, the differences between $\Delta\nu_{as\text{-}s}$ were found in order of 144, 144, 175 and 177 cm^{-1}. These results are strong evidence for the binding behaviour of coumarilate ligand as monoanionic monodentate for compounds **1** and **2**, whereas monoanionic bidentate for compounds **3** and **4**.

In the light of the thermal analysis data, the thermal decomposition of the complexes was started firstly by the elimination of aqua ligands, continued by the combustion of coumarilate which is an organic group. At the end, the elimination was ended by the remaining of the related metal oxides.

Supplementary material

Crystallographic data for the structural analysis have been deposited with the Cambridge Crystallographic Data Centre, CCDC No. 1458972 for **1**, 1458973 for **2** and 1458974 for **4**. Copies of this information may be obtained free of charge from the Director, CCDC, 12 Union Road, Cambridge CB2 1EZ, UK (Fax: +44-1223-336033; E-mail: deposit@ccdc.cam.ac.uk or www: http://www.ccdc.cam.ac.uk).

Acknowledgements This work has been supported by Hitit University Scientific Research Unit (Project No: FEF19004.15.005).

References

1. Gilchrist TL. Heterocyclic chemistry. Harlow: Longman Group UK Limited; 1985.
2. Hattori M, Hada S, Watahiki A, Ihara H, Shu YZ, Kakiuchi N, Mizuno T, Namba T. Studies on dental caries prevention by traditional medicines. X. Antibacterial action of phenolic components from mace against *Streptococcus mutans*. Chem Pharm Bull. 1986;34:3885–93.
3. Erber S, Ringshandl R, von Angerer E. 2-Phenylbenzo[b]furans: relationship between structure, estrogen receptor affinity and cytostatic activity against mammary tumor cells. Anticancer Drug Des. 1991;6:417–26.
4. Cui B, Chai H, Reutrakul V, Farnsworth NR, Cordell GA, Pezzutto JM, Kinghorn AD. Novel cytotoxic 1H-cyclopenta[b]-benzofuran lingnans from *Aglaia elliptica*. Tetrahedron. 1997;53:17625–32.
5. Lee SK, Cui B, Mehta RR, Kinghorn AD, Pezzutto JM. Cytostatic mechanism and antitumor potential of novel 1H-cyclopenta[b]benzofuran lignans isolated from *Aglaia elliptica*. Chem Biolog Interact. 1998;115:215–28.
6. Kodama I, Kamiya K, Toyama J. Amiodarone: ionic and cellular mechanisms of action of the most promising class III agent. Am J Card. 1999;84:20R–8R.
7. Hayakawa I, Shioya R, Agatsuma T, Furukawa H, Naruto S, Sugano Y. 4-Hydroxy-3-methyl-6-phenylbenzofuran-2-carboxylic acid ethyl ester derivatives as potent anti-tumor agents. Bioorg Med Chem Lett. 2004;14:455–8.
8. Hwang BY, Su BN, Chai H, Mi Q, Kardono LB, Afriastini JJ, Riswan S, Santarsiero BD, Mesecar AD, Wild R, Fairchild CR, Vite GD, Rose WC, Farnsworth NR, Cordell GA, Pezzutto JM, Swanson SM, Kinghorn AD. Silvestrol and episilvestrol, potential anticancer rocaglate derivatives from *Aglaia silvestris*. J Org Chem. 2004;69:3350–8.
9. Masche UP, Rentsch KM, von Felten A, Meier PJ, Fattinger KE. No clinically relevant effect of lornoxicam intake on acenocoumarol pharmacokinetics and pharmacodynamics. Eur J Clin Pharm. 1999;54(11):865–8.
10. Karaliota A, Kretsi O, Tzougraki C. Synthesis and characterization of a binuclear coumarin-3-carboxylate copper(II) complex. J Inorg Biochem. 2001;84:33–7.
11. Kossakowski J, Krawiecka M, Kuran B, Stefanska J, Wolska I. Synthesis and preliminary evaluation of the antimicrobial activity of selected 3-benzofurancarboxylic acid derivatives. Molecules. 2010;15:4737–49.
12. Kossakowski J, Ostrowska K, Hejchman E, Wolska I. Synthesis and structural characterization of derivatives of 2- and 3-benzo[b]furan carboxylic acids with potential cytotoxic activity. Farmaco. 2005;60:519–27.
13. Kowalewska H, Kwiecien H, Smist M, Wrzesniewska A. Synthesis of new benzofuran-2-carboxylic acid derivatives. J Chem. 2013;. doi:10.1155/2013/183717.
14. Köse DA, Öztürk B, Şahin O, Büyükgüngör O. Mixed ligand complexes of coumarilic acid/nicotinamide with transition metal complexes. J Therm Anal Calorim. 2014;115:1515–24.
15. Drzewiecka A, Koziol AE, Klepka MT, Wolska A, Jimenez-Pulido SB, Lis T, Ostrowska K, Struga M. Two coordination modes around the Cu(II) cations in complexes with benzo[b]furancarboxylic acids. Chem Phys Lett. 2013;559:41–5.
16. Limaye DB, Sathe NR. Syntheses of 6-hydroxy-7-acylcoumarones. I. 6-Hydroxy-7-acetyl-3-methylcoumarone. Rasayanam. 1936;1:48–54.
17. Shah NM, Shah PM. Hydroxy-acyl-cumarone, III. Friessche Verschiebung von 5-substituierten 6-acyloxy-3-methyl-cumarilsäuren. Chem Ber. 1960;93:18–24.
18. Zawadowski T, Kossakowski J, Rechowicz P. Synthesis of 2-methyl-5-hydroxy-6-acetylbenzofuran-3-carboxylic acid and its derivatives. Rocz Chem Ann Soc Chim Polonorum. 1977;51:159–62.
19. Ng SW. Coordination complexes of triphenyltin coumarin-3-carboxylate with O-donor ligands: (coumarin-3-carboxylato) triphenyltin-L (L = ethanol, diphenylcyclopropenone and quinoline *N*-oxide) and bis[(coumarin-3-carboxylato)triphenyltin]-L(L = triphenylphosphine oxide and triphenylarsine oxide). Acta Cryst. 1999;C55:523–31.
20. Castellani CB, Carugo O. Studies on fluorescent lanthanide complexes. New complexes of lanthanides(III) with coumarinic-3-carboxylic acid. Inorg Chim Acta. 1989;159:157–61.
21. Mihaylov TZ, Trendafilova N, Kostova I, Georgieva I, Bauer G. DFT modeling and spectroscopic study of metal–ligand bonding in La(III) complex of coumarin-3-carboxylic acid. Chem Phys. 2006;327:209–19.
22. Georgieva I, Trendafilova N, Aquino AJA, Lischka H. Theoretical study of metal–ligand interaction in Sm(III), Eu(III), and Tb(III) complexes of coumarin-3-carboxylic acid in the gas phase and solution. Inorg Chem. 2007;46(25):10926–36.
23. Georgieva I, Trendafilova N, Creaven BS, Walsh M, Noble A, McCann M. Is the C=O frequency shift a reliable indicator of coumarin binding to metal ions through the carbonyl oxygen? Chem Phys. 2009;365(1–2):69–79.
24. Roh SG, Baek NS, Hong KS, Kim HK. Synthesis and photophysical properties of luminescent lanthanide complexes based on coumarin-3-carboxylic acid for advanced photonic applications. Bull Korean Chem Soc. 2004;25(3):343–4.
25. Creaven BS, Devereux M, Georgieva I, Karcz D, McCann M, Trenddafilova N, Walsh M. Molecular structure and spectroscopic studies on novel complexes of coumarin-3-carboxylic acid with Ni(II), Co(II), Zn(II) and Mn(II) ions based on density functional theory. Spectrochim Acta A. 2011;84(1):275–85.
26. Icbudak H, Heren Z, Kose DA, Necefoglu H. bis(nicotinamide) and bis(*N*,*N*-diethylnicotinamide) p-hydroxybenzoate complexes of N^{I}(II), Cu(II) and Zn(II). Spectrothermal studies. J Therm Anal Calorim. 2004;76:837–51.
27. Sheldrick GM. A short history of SHELX. Acta Cryst. 2008;A64:112–22.
28. Farrugia LJ. WinGX suite for small-molecule single-crystal crystallography. J Apply Cryst. 1999;32:837–8.
29. Mercury, version 3.0; CCDC, available online via ccdc.cam.ac.uk/products/mercury.
30. Spek AL. PLATON—a multipurpose crystallographic tool. Utrecht: Utrecht University; 2005.
31. Köse DA, Şahin O, Büyükgüngör O. Synthesis, spectral, thermal, magnetic and structural study of diaquabis(salicylato-κO)bis(*N*,*N*-diethylnicotinamide-κN)cobalt(II). Eur Chem Bull. 2012;1(6):196–201.

32. Köse DA, Ay AN, Şahin O, Büyükgüngör O. A mononuclear Zn(II) complex of mixed ligands with both fivefold- and sixfold-coordinations in the same framework. J Iran Chem Soc. 2012;9(4):591–7.
33. Köse DA, Necefoğlu H, Şahin O, Büyükgüngör O. Synthesis, structural, spectroscopic characterization and structural comparison of 3-hydroxybenzoate and nicotinamide/*N*,*N*-diethylnicotinamide mixed ligand complexes with Zn(II). J Therm Anal Calorim. 2012;110(3):1233–41.
34. Nakamoto K. Infrared and Raman spectra of inorganic and coordination compounds. Toronto: Wiley; 1997.
35. Köse DA, Gökçe G, Gökçe S, Uzun I. Bis(*N*,*N*-diethyl nicotinamide) *p*-chlorobenzoate complexes of Ni(II), Zn(II) and Cd(II), synthesis and characterization. J Therm Anal Calorim. 2009;95(1):247–51.